Available online at www.sciencedirect.com
SCIENCE DIRECT®
Journal of Sound and Vibration 282 (2005) 111–124
JOURNAL OF SOUND AND VIBRATION
www.elsevier.com/locate/jsvi

A study of random vibration characteristics of the quarter-car model

Semiha Türkay, Hüseyin Akçay*

Department of Electrical and Electronics Engineering, Anadolu University, 26470 Eskişehir, Turkey

Received 7 July 2003; accepted 16 February 2004
Available online 12 October 2004

Abstract

In this paper, the quarter-car model is used to study the response of the vehicle to profile imposed excitation with randomly varying traverse velocity and variable vehicle forward velocity. Root-mean-square response of the vehicle to white and colored noise velocity road inputs is analyzed. In the latter case, a recently developed subspace-based identification algorithm is used to design a linear shape filter with output spectrum matching the measured road spectrum. The linear shape filter is used in constructing charts that illustrate the trade-offs among the passenger comfort, the road-holding, and the suspension travel as functions of the vehicle forward velocity.

1. Introduction

High-quality simulation of vehicle vibration can only be done with three-dimensional models. Since the equations of motion for systems with many degrees of freedom can be derived from computerized algorithms, a good approximation to real vehicle dynamics is possible. However, a detailed analysis of the ride performance limitations of active and passive suspension systems needs detailed road modeling analysis and the performance indexes employed in optimal control laws require road elevations to be known. Thus, it is important to predict vehicle dynamic response using realistic road models.

*Corresponding author. Tel.: +90-222-335-0580-6459; fax: +90-222-323-9501.
E-mail address: huakcay@anadolu.edu.tr (H. Akçay).

0022-460X/$ - see front matter © 2004 Elsevier Ltd. All rights reserved.
doi:10.1016/j.jsv.2004.02.049

A realistic road model must take into account the correlation between the different axles and the correlation between parallel tracks. It is generally agreed that typical road surfaces may be considered as realizations of homogeneous and isotropic two-dimensional Gaussian random processes and these assumptions make it possible to completely describe a road profile by a single-power spectral density evaluated from any longitudinal track [1,2]. Then, the spectral description of the road, together with a knowledge of traversal velocity and of the dynamic properties of the vehicle, provide a response analysis which will describe the response of the vehicle expressed in terms of displacement, acceleration, or stress [3].

Active control of vehicle suspensions has been the subject of considerable investigation since the late 1960s; see, for example, [4–6] and the references therein. Studies concerning the limitations and potential benefits of active suspensions [7–9] have shown that suspension controllers that focus on a fixed performance measure offer a limited improvement in performance over conventional passive suspensions, when the improvement is assessed over the whole range of road conditions. During driving the character of dynamical interaction between the road and the vehicle changes dramatically depending on road surface and vehicle velocity. These changes must be taken into account to ensure optimal (or sub-optimal) acting of the system in every condition. In order to realize the full potential of active suspensions, the controller should have the capability of adapting to changing road environments [10,11].

In this paper, first an identification algorithm developed in Ref. [12] is used to model the power spectrum of a typical road profile by a rational function of reasonably low order from corrupted spectrum samples. The goal here is to use this approximation for the design of a linear shaping filter with a white noise input. Once such an approximation is made, the vehicle control problem can be formulated in standard form. Then, the modeled road spectrum is used in the quarter-car model to study the random vibration of the vehicle due to road unevenness and variable vehicle velocity. In earlier work on the analysis of vehicle response, the vehicle velocity was usually considered as constant. The effect of the change in the vehicle velocity in stationary response to the profile imposed excitation was investigated in Refs. [13,14].

The preliminary results show that the first-order road displacement model in Ref. [3] is too simple to predict the random vibration of the vehicle. The trade-offs between the passenger comfort, the suspension travel, and the road-holding are also illustrated for a range of vehicle velocities and shape filter orders. The best results are obtained with high orders. The integrated white noise approximation to the road displacement spectrum [7] yields more accurate results than those of the low-order fit. But at high speeds, this approximation is also seen to be unacceptable.

2. The quarter-car model with random road inputs

In this section, the quarter-car model is used to study the response of the vehicle to random road inputs. First, a linear two-degree-of-freedom car model is reviewed. Then, the response of the vehicle to random road disturbances is analyzed by treating them either as white noise velocity inputs or colored noise inputs. It is recognized that the quarter-car representation is too simple for performing a comprehensive analysis of the ride motions of the vehicle. However, even with this simplified representation, significant insight into the problem can be gained without greatly complicating the analysis.

2.1. The equations of motion in state-space form

A two-degree-of-freedom quarter-car model is shown in Fig. 1. In this model, the sprung and unsprung masses corresponding to the one corner of the vehicle are denoted respectively by m_s and m_u. The suspension system is represented by a linear spring of stiffness K_s and a linear damper with a damping rate C_s, while the tire is modeled by a linear spring of stiffness K_T. Since damping in the tire is typically very small, it is neglected in this study. The parameter values chosen for this study are shown in Table 1. They are typical for a lightly damped passenger car.

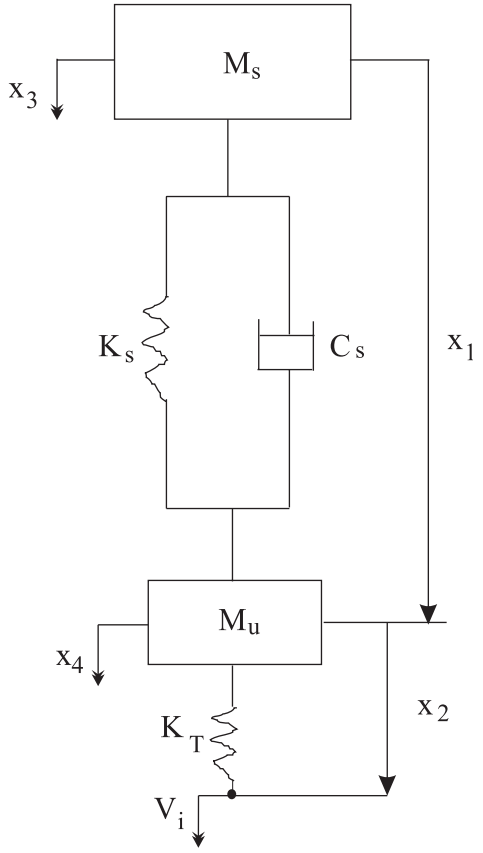

Fig. 1. The quarter-car model of the vehicle.

Table 1
The vehicle system parameters for the quarter-car model [7]

Sprung mass	m_s	240 kg
Unsprung mass	m_u	36 kg
Damping coefficient	C_s	980 Ns/m
Secondary suspension stiffness	K_s	16,000 N/m
Primary suspension stiffness	K_T	160,000 N/m

The vehicle is assumed to travel at a constant forward speed denoted by v over a random road surface. It is also assumed that the tire behaves as a point-contact follower that is in contact with the road at all times. Then, the equations of motion in the state-space configuration take the form

$$\begin{bmatrix} \dot{x}_1 \\ \dot{x}_2 \\ \dot{x}_3 \\ \dot{x}_4 \end{bmatrix} = \begin{bmatrix} 0 & 0 & 1 & -1 \\ 0 & 0 & 0 & 1 \\ -K_s/m_s & 0 & -C_s/m_s & C_s/m_s \\ K_s/m_u & -K_T/m_u & C_s/m_u & -C_s/m_u \end{bmatrix} \begin{bmatrix} x_1 \\ x_2 \\ x_3 \\ x_4 \end{bmatrix} + \begin{bmatrix} 0 \\ -1 \\ 0 \\ 0 \end{bmatrix} V_i,$$

$$\dot{\mathbf{X}} = \mathbf{A}\mathbf{X} + \mathbf{B}V_i, \tag{1}$$

where V_i is the velocity input and the state variables are defined as follows:

x_1: the distance between the sprung and unsprung masses (suspension travel);
x_2: the distance between the unsprung mass and the road surface (tire deflection);
x_3: the sprung mass absolute velocity;
x_4: the unsprung mass absolute velocity.

The primary objective of this study is to investigate trade-offs between the vibration isolation, the suspension travel, and the road-holding characteristics of the vehicle due to road surface unevenness and the changes in the velocity of the vehicle. Hence, the vehicle response variables that need to be examined are:

$\dot{x}_3$: the vertical acceleration of the sprung mass;
x_1: the suspension travel;
x_2: the tire deflection.

Thus, the output can be expressed in terms of the state vector as

$$\mathbf{Y} = \begin{bmatrix} -K_s/m_s & 0 & -C_s/m_s & C_s/m_s \\ 1 & 0 & 0 & 0 \\ 0 & 1 & 0 & 0 \end{bmatrix} \begin{bmatrix} x_1 \\ x_2 \\ x_3 \\ x_4 \end{bmatrix} = \mathbf{C}\mathbf{X}. \tag{2}$$

It should be noted that the choice of state variables is rather arbitrary; and different choices yield the same transfer function matrix $\mathbf{G}(s) = \mathbf{C}(s\mathbf{I}_4 - \mathbf{A})^{-1}\mathbf{B}$ from V_i to $\mathbf{Y}$, where $\mathbf{I}_n$ is the $n \times n$ identity matrix.

Passenger comfort requires $\dot{x}_3$ to be as small as possible while compactness of rattle space, good handling characteristics, which are needed during steering maneuvers, and improved road-holding quality require x_1 and x_2 to be kept small. With the passive suspension configuration of Fig. 1, it is a well-known fact that these objectives cannot be met simultaneously [8]. During cornering, the vehicle is subjected to centrifugal forces. The centrifugal forces cause rolling of the vehicle. In order to maintain the rolling at tolerable levels, one must keep K_s sufficiently large. Thus, the only

parameter that can be altered in an optimization study is C_s: decreasing C_s decreases $\dot{x}_3$ whereas it increases x_1 and x_2. The conflicting three goals can be attained up to a certain extent by employing an active or semi-active suspension instead of the passive suspension in Fig. 1 [5,7,9,15–18].

2.2. Description of road surface roughness

The description of the road surface as a realization of a stationary random process will enable the response of a vehicle traversing a given road to be determined by means of the accepted techniques of the theory of random vibration. In the particular case of stationary random excitations with a normal distribution and zero-mean value, it is only necessary to compute from the time histories of the excitations their second-order moments, or in effect their spectral densities, to obtain a sufficient statistical description of the excitation process. Thus a spectral description of the road, together with a knowledge of traversal velocity and of the dynamic properties of the vehicle, will provide a response analysis.

In Fig. 2 [1], spectral density of a typical road; the split power-law approximation

$$S_{\mathrm{sp}}(n) = \begin{cases} \kappa |n/n_0|^{-2\delta_1}, & 0 < |n| < n_0, \\ \kappa |n/n_0|^{-2\delta_2}, & n_0 \leqslant |n| < \infty \end{cases}$$

obtained by trial and error for the values $\kappa = 0.76 \times 10^{-5}$, $\delta_1 = 1.6$, and $\delta_2 = 1.1$; and the integrated white noise approximation [7] defined by

$$S_{\mathrm{iw}}(n) = \kappa (n_0/n)^2 \tag{3}$$

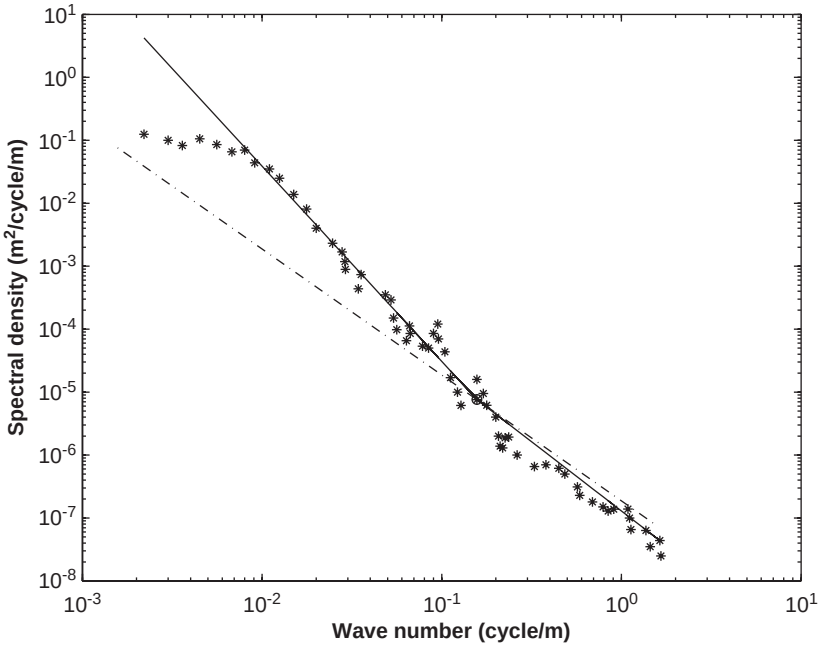

Fig. 2. The spectral data and its approximate modeling: ∗ data, — split power law, –·– integrated white noise.

are shown where n denotes the (spatial) frequency measured in cycles/m. Both the approximations are made to match the spectral data at the (spatial frequency) $n_0 = 0.15708$ cycles/m. It is clear that the fit by the integrated white noise modeling is rather poor; in particular at the frequencies below n_0. The problem with the split power approximation is that it cannot be generated by *linear shape filters*. Hence, it is not suitable for simulating the response of the vehicle. Besides, it is unbounded at the zero frequency.

The purpose of modeling a power spectrum by a rational function of reasonably low order is to use this approximation for the design of a linear shape filter with a white noise input. Then, the identified road spectrum is used in the quarter-car model to study the response of the vehicle to random road inputs.

2.3. White noise velocity input

Note that $S_{\mathrm{iw}}(n)$ in Eq. (3) is the power spectral density of $\xi(l)$ in the road model

$$\frac{\mathrm{d}}{\mathrm{d}l}\,\xi(l) = 2\pi n_0\sqrt{\kappa}v(l), \tag{4}$$

where $v(l)$ is a zero-mean (spatial) white noise process with a covariance function

$$\mathscr{E}\{v(l)v(l+\tau)\} = R_v(\tau) = \delta(\tau). \tag{5}$$

Here $\mathscr{E}(\cdot)$ denotes the expected value and $\delta(\tau)$ is the unit impulse function. Thus, the road displacement $\xi(l)$ is modeled by an integrated white-noise process. In this model, the road profile is adjusted by changing κ and n_0 in Eq. (3). Plugging $l = vt$, $\eta(t) = v(vt)$, and $\zeta(t) = \xi(vt)$ in Eq. (4) and applying the chain rule of differentiation, we get

$$V_i = \frac{\mathrm{d}}{\mathrm{d}t}\,\zeta(t) = 2\pi n_0 v\sqrt{\kappa}\eta(t), \tag{6}$$

where v is the vehicle forward velocity measured in m/s and $\eta(t)$ is a zero-mean (temporal) white noise process with the covariance function:

$$R_\eta(\tau) = (1/v)\delta(\tau). \tag{7}$$

Thus, from Eqs. (1), (2), (6), and (7)

$$\begin{aligned}\dot{\mathbf{X}}(t) &= \mathbf{A}\mathbf{X}(t) + 2\pi n_0\sqrt{v\kappa}\mathbf{B}\tilde{\eta}(t),\\ \mathbf{Y}(t) &= \mathbf{C}\mathbf{X}(t),\end{aligned} \tag{8}$$

where $\tilde{\eta}(t)$ is a zero-mean (temporal) white noise process with the covariance function

$$R_{\tilde{\eta}}(\tau) = \delta(\tau). \tag{9}$$

Recall that for a wide-sense stationary random process $z(t)$, $\mathscr{E}\{z^2(t)\}$ does not depend on t and it equals $R_z(0)$. The square-root of $R_z(0)$ is called the *root-mean square* (rms) of $z(t)$ and is a measure of vibration level experienced by the vehicle. If, for example, V_i is assumed to be a zero-mean, wide-sense stationary random process, then the components of $\mathbf{Y}(t)$ will also be zero-mean, wide-sense stationary random processes with constant standard deviations which equal to the rms values of the components of $\mathbf{Y}(t)$.

The state covariance matrix $\mathbf{R}_{\mathbf{X}}(0)$ is obtained by solving the *Lyapunov equation*:

$$\mathbf{A}\mathbf{R}_{\mathbf{X}}(0) + \mathbf{R}_{\mathbf{X}}(0)\mathbf{A}^{\mathrm{T}} + v\kappa(2\pi n_0)^2\mathbf{B}\mathbf{B}^{\mathrm{T}} = 0. \tag{10}$$

Then, $\mathbf{R}_{\mathbf{Y}}(0)$ and the output spectrum of $\mathbf{Y}$ are computed from Eq. (8) as

$$\mathbf{R}_{\mathbf{Y}}(0) = \mathbf{C}\mathbf{R}_{\mathbf{Y}}(0)\mathbf{C}^{\mathrm{T}} \tag{11}$$

and

$$\mathbf{S}_{\mathbf{Y}}(\hat{n}) = \int_{-\infty}^{\infty} \mathbf{R}_{\mathbf{Y}}(\tau)\mathrm{e}^{-\mathrm{j}2\pi\hat{n}}\,\mathrm{d}\tau = v\kappa(2\pi n_0)^2\mathbf{G}(\mathrm{j}2\pi\hat{n})\mathbf{G}^{\mathrm{T}}(-\mathrm{j}2\pi\hat{n}), \tag{12}$$

where $\hat{n}$ denotes the (temporal) frequency measured in Hz. The square roots of the elements in the diagonal of $\mathbf{R}_{\mathbf{Y}}(0)$ equal to the rms values of $\dot{x}_3$, x_1, and x_2, respectively.

2.4. Colored noise velocity input

Let

$$\begin{aligned} \dot{\mathbf{Z}}(l) &= \widetilde{\mathbf{A}}\mathbf{Z}(l) + \widetilde{\mathbf{B}}v(l), \\ \xi(l) &= \widetilde{\mathbf{C}}\mathbf{Z}(l), \end{aligned} \tag{13}$$

where $\xi(l)$ denotes the road displacement at the longitudinal coordinate l and $v(l)$ is a zero-mean (spatial) white noise process with a covariance function satisfying Eq. (5). In Eq. (13), the eigenvalues of $\widetilde{\mathbf{A}} \in \mathscr{R}^{m\times m}$ are restricted inside the unit circle centered at the origin. The transfer function

$$\widetilde{G}(s) = \widetilde{\mathbf{C}}(s\mathbf{I}_m - \widetilde{\mathbf{A}})^{-1}\widetilde{\mathbf{B}} \tag{14}$$

is called the *spectral factor* of the power spectrum of ξ computed from Eqs. (5) and (14) as

$$S_{\xi}(n) = |\widetilde{G}(\mathrm{j}2\pi n)|^2.$$

In the design of a linear shape filter, one aims to match given spectral data as closely possible as by suitably selecting the state-space parameters $(\widetilde{\mathbf{A}}, \widetilde{\mathbf{B}}, \widetilde{\mathbf{C}})$ in Eq. (13). Provided that $S_{\xi}(n)$ is a smooth function, this aim can be achieved for large filter orders. In the next section, estimation results of an identification algorithm that uses given spectral data and yields a state-space realization of $\widetilde{G}(s)$ will be presented.

Applying the chain rule of differentiation to $l = vt$, we can transform Eq. (13) into the time domain as follows:

$$\begin{aligned} \dot{\mathbf{U}}(t) &= v\widetilde{\mathbf{A}}\mathbf{U}(t) + \sqrt{v}\widetilde{\mathbf{B}}\widetilde{\eta}(t), \\ w(t) &= \widetilde{\mathbf{C}}\mathbf{U}(t), \end{aligned} \tag{15}$$

where $\mathbf{U}(t) = \mathbf{Z}(vt)$, $w(t) = \xi(vt)$, and $\widetilde{\eta}(t)$ is a zero-mean (temporal) white noise process with a covariance function as in Eq. (9). The output $w(t)$ of the time-domain shape filter (15) is related to V_i by the equation

$$V_i = \dot{w}(t) = v\widetilde{\mathbf{C}}\widetilde{\mathbf{A}}\mathbf{U}(t) + \sqrt{v}\widetilde{\mathbf{C}}\widetilde{\mathbf{B}}\widetilde{\eta}(t). \tag{16}$$

Thus, from Eqs. (1), (2), (15), and (16) the equations of the motion of the vehicle can be written in state-space form as

$$\frac{\mathrm{d}}{\mathrm{d}t}\widehat{\mathbf{X}}(t) = \widehat{\mathbf{A}}\widehat{\mathbf{X}}(t) + \widehat{\mathbf{B}}\widetilde{\eta}(t),$$
$$\mathbf{Y}(t) = \widehat{\mathbf{C}}\widehat{\mathbf{X}}(t), \tag{17}$$

where

$$\widehat{\mathbf{X}} = \begin{bmatrix}\mathbf{X}\\ \mathbf{U}\end{bmatrix}, \quad \widehat{\mathbf{A}} = \begin{bmatrix}\mathbf{A} & v\mathbf{B}\widetilde{\mathbf{C}}\widetilde{\mathbf{A}}\\ 0 & v\widetilde{\mathbf{A}}\end{bmatrix},$$
$$\widehat{\mathbf{B}} = \sqrt{v}\begin{bmatrix}\mathbf{B}\widetilde{\mathbf{C}}\widetilde{\mathbf{B}}\\ \widetilde{\mathbf{B}}\end{bmatrix}, \quad \widehat{\mathbf{C}} = [\mathbf{C} \quad 0]. \tag{18}$$

As in Eqs. (10) and (11), the state and the output covariance matrices $\mathbf{R}_{\hat{\mathbf{X}}}(0)$ and $\mathbf{R}_{\mathbf{Y}}(0)$ are obtained from

$$\widehat{\mathbf{A}}\mathbf{R}_{\hat{\mathbf{X}}}(0) + \mathbf{R}_{\hat{\mathbf{X}}}(0)\widehat{\mathbf{A}}^{\mathrm{T}} + \widehat{\mathbf{B}}\widehat{\mathbf{B}}^{\mathrm{T}} = 0,$$
$$\mathbf{R}_{\mathbf{Y}}(0) = \widehat{\mathbf{C}}\mathbf{R}_{\hat{\mathbf{X}}}(0)\widehat{\mathbf{C}}^{\mathrm{T}}. \tag{19}$$

Moreover, $\mathbf{S}_{\mathbf{Y}}(\widehat{n}) = \widehat{\mathbf{G}}(\mathrm{j}2\pi\widehat{n})\widehat{\mathbf{G}}^{\mathrm{T}}(-\mathrm{j}2\pi\widehat{n})$ where

$$\widehat{\mathbf{G}}(s) = \widehat{\mathbf{C}}(s\mathbf{I}_{n+m} - \widehat{\mathbf{A}})^{-1}\widehat{\mathbf{B}}.$$

2.5. Identification of road spectra

The problem of designing linear shape filters from noisy samples of power spectrum is discussed in Ref. [12]. In this work, a subspace-based frequency-domain algorithm for the identification of power spectra from nonuniformly spaced measurements is developed. The details are omitted. When applied to the spectral data plotted in Fig. 2, this algorithm yields the following linear shape filters:

$$\widetilde{G}_8(s) = \Lambda(s)\ 4.35 \times 10^{-7} \prod_{k=1}^{7} \frac{s + z_k}{s + p_k}, \tag{20}$$

where $p_{1,2} = 0.045 \pm 0.163\mathrm{j}$, $p_{3,4} = 0.007 \pm 0.157\mathrm{j}$, $p_{5,6} = 0.043 \pm 0.050\mathrm{j}$, $p_7 = 0.007$; $z_1 = 4686$, $z_2 = 0.603$, $z_{3,4} = 0.031 \pm 0.163\mathrm{j}$, $z_{5,6} = 0.009 \pm 0.154\mathrm{j}$, $z_7 = 0.0154$; and the roll-off factor $\Lambda(s)$ is defined by

$$\Lambda(s) = \frac{10}{s + 10}$$

and

$$\widetilde{G}_2(s) = \Lambda(s)\ 0.83876\ \frac{s + 0.014}{s + 0.042}. \tag{21}$$

The transfer functions $\Lambda^{-1}(s)\widetilde{G}_2(s)$ and $\Lambda^{-1}(s)\widetilde{G}_8(s)$ are the *spectral factors* delivered by the algorithm in Ref. [12] by taking noise covariance there equal to the road power

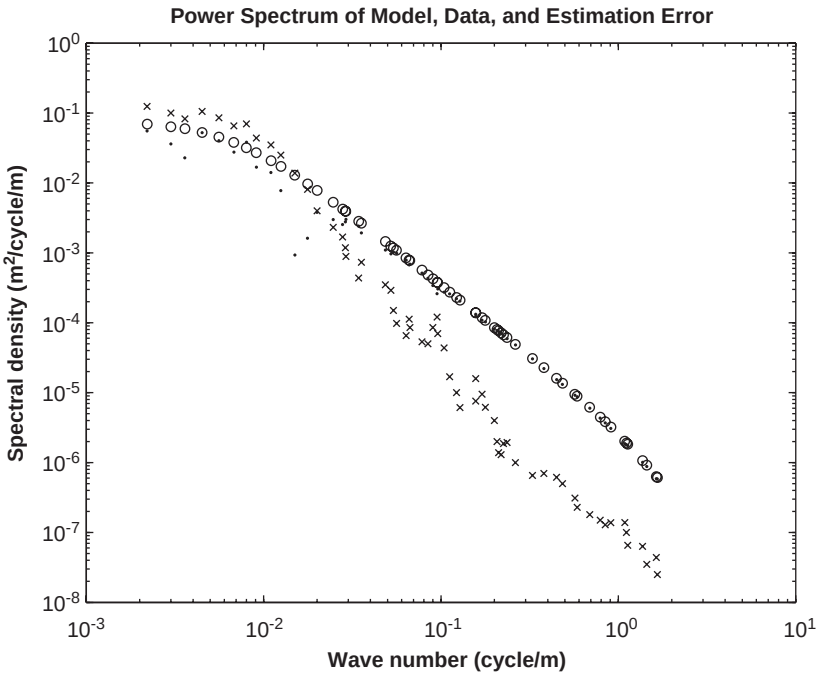

Fig. 3. The spectral data, its approximate modeling by a shape filter of order 2, and the estimation error: $*$ data, o $S_{\xi}(n)$, $\cdot$ error.

spectrum. The roll-off factor slightly affects the spectral factors due to the bandwidth of the spectral data.

In Figs. 3 and 4, the estimation results are plotted for the shape filters in Eqs. (20) and (21). In the figures, the estimation error is defined as the absolute value of the difference between the data and the estimated road power spectrum. In the numerical study, filter orders between two and eight have been tried; but best results were obtained for $m = 8$.

Fig. 4 demonstrates that the eighth-order shape filter is capable of capturing the road dynamics in the entire bandwidth considered. On the other hand, the output spectrum of the second-order shape filter is rather erratic. Henceforth, it is not suitable model for road profiles. Thus, in the modeling of road spectra high-order shape filters are suggested. This conclusion will be supported by a study of the trade-offs in the following section.

3. Stochastic response and the trade-offs

In Fig. 5, the rms vertical acceleration of the vehicle subjected to white and colored noise velocity inputs with filter orders $m = 2$ and 8 is plotted as a function of the vehicle velocity. The rms values were computed by solving Eqs. (10), (11) and (19). This figure reveals that up to 108 km/h the integrated white noise and the eighth-order shape filter approximations yield

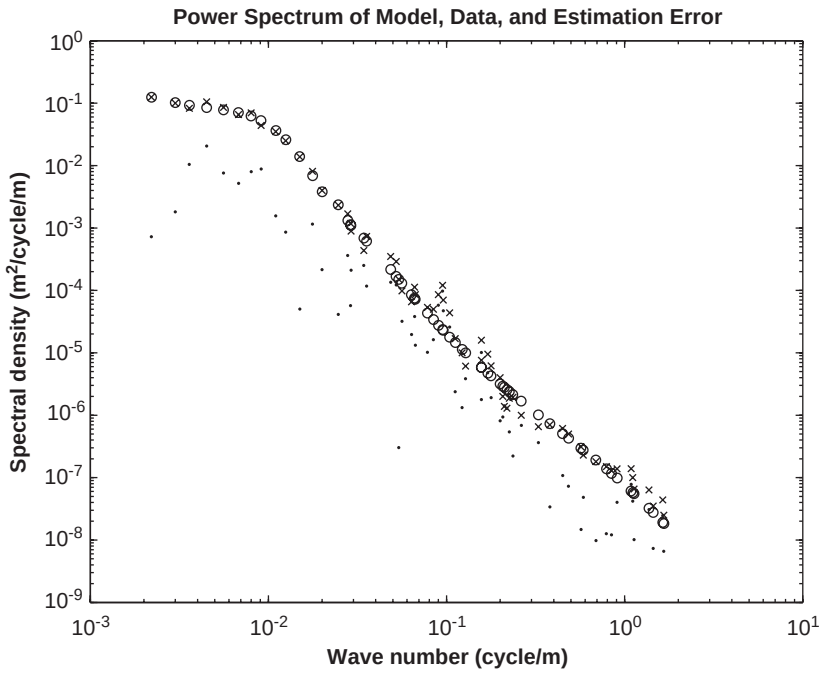

Fig. 4. The spectral data, its approximate modeling by a shape filter of order 8, and the estimation error: $*$ data, o $S_{\xi}(n)$, $\cdot$ error.

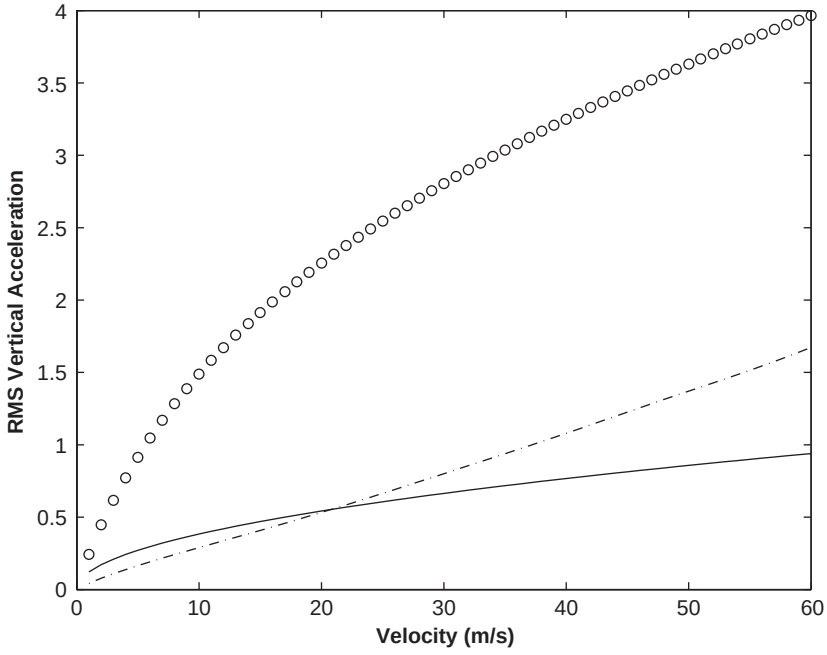

Fig. 5. The rms vertical acceleration of the vehicle subjected to white and colored noise velocity inputs for filter orders $m = 2$ and 8 as a function of the vehicle velocity: o $m = 2$, – $m = 8$, – white noise.

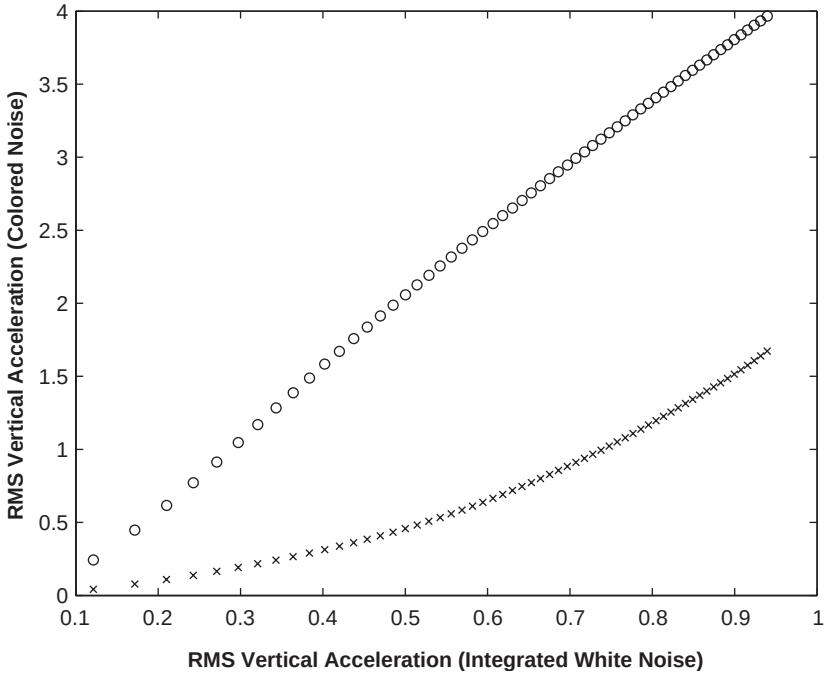

Fig. 6. The relationship between the rms vertical accelerations of the vehicle subject to the white and colored noise velocity inputs with shape filters as a function of v: o $m = 2$, x $m = 8$.

agreeable responses while the response due to the second-order approximation departs remarkably from the others in all frequencies. Similar results have been obtained for the rms suspension travel versus the velocity and the rms tire deflection versus the velocity curves.

In Fig. 6, for shape filters of orders $m = 2$ and 8 the rms vertical acceleration of the vehicle subject to colored noise velocity input is plotted versus that of the vehicle excited by white noise velocity input for the vehicle forward velocity ranging from 0 to 60 m/s. These curves are drawn by varying v. This figure indicates that if the eighth-order shape filter whose output spectrum matches the road spectrum as close as possible is taken as a basis for comparison, then the second-order shape filter is not suitable for a study of vehicle random vibrations. Interestingly, the integrated white noise approximation to the road displacement spectrum yields more accurate results than those of the second-order fit. But at high speeds, in particular for $v \geqslant 30$ m/s, this approximation ceases to be acceptable.

In Figs. 7 and 8, at $v = 108$ km/h the trade-off curves for the colored noise velocity input case are displayed with the integrated white noise displacement input. These curves are drawn by varying C_s and fixing the others in Table 1. The trade-off curves are similar to the trade-off curves in Ref. [7]. Once more, it is acknowledged that the second-order shape filter is not suitable and the integrated white noise is somewhat appropriate for the modeling of the road displacement spectrum. Note with the integrated white noise road displacement model that the vehicle forward velocity does not influence the shapes of the curves.

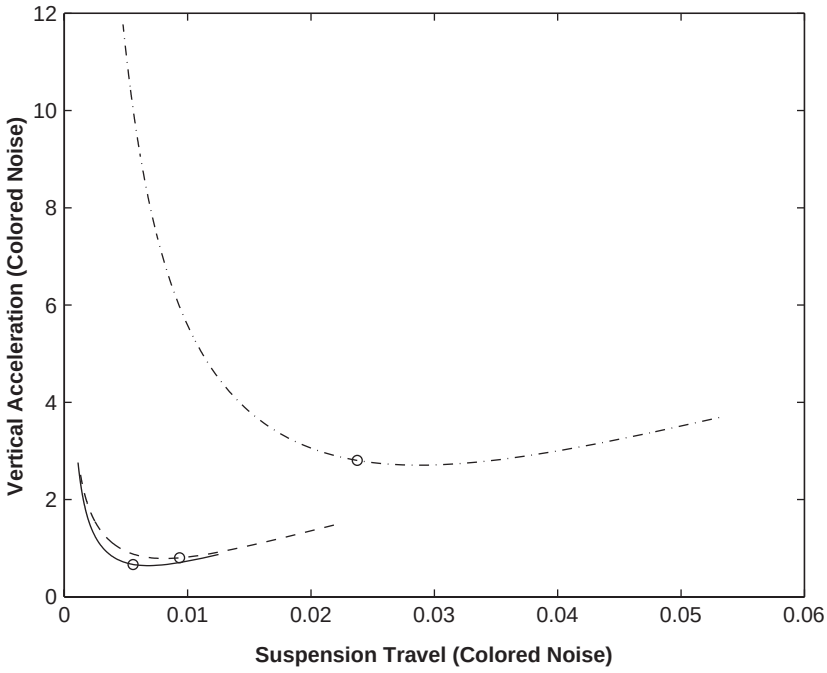

Fig. 7. The relationship between the rms vertical acceleration and the rms suspension travel of the vehicle subject to white and colored noise velocity inputs for filter orders $m = 2$ and 8 at $v = 108$ km/h as a function of C_s: — white noise, – $m = 2$, - - $m = 8$, $C_s = 980$ is denoted by o.

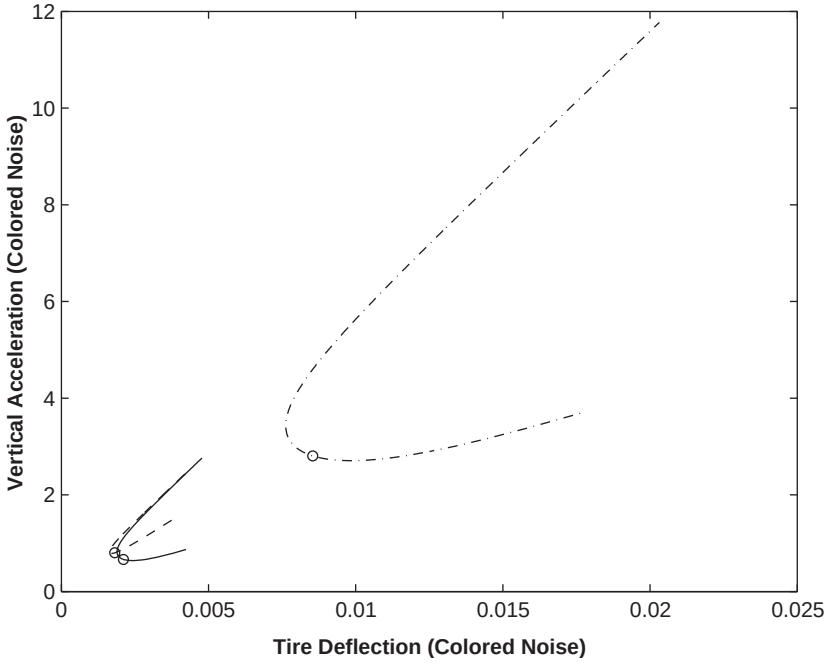

Fig. 8. The relationship between the rms vertical acceleration and the rms tire deflection of the vehicle subject to white and colored noise velocity inputs for filter orders $m = 2$ and 8 at $v = 108$ km/h as a function of C_s: — white noise, – $m = 2$, - - $m = 8$, $C_s = 980$ is denoted by o.

4. Conclusions

In this paper, a quarter-car model was used to study the response of the vehicle to random road excitations. The response of the vehicle to random road disturbances was analyzed by treating them either as white noise velocity inputs or colored noise inputs. In the latter case, the inputs were generated as the output of a linear shape filter derived directly from the measurements of the road profile power spectrum by an identification algorithm. The analysis has shown that second-order shape filters are too simple to predict the behavior of the vehicle subjected to random excitations. The trade-offs between the variables of interest were also illustrated for a specific road profile spectrum and a range of velocities with two shape filters. The best results were obtained for a high-order shape filter. The integrated white noise approximation to the road displacement spectrum yielded more accurate results than those of the second-order fit. But at high speeds, in particular for $v \geqslant 100\,\mathrm{km/h}$, this approximation was also seen to be unacceptable.

References

[1] C.J. Dodds, J.D. Robson, The description of road surface roughness, *Journal of Sound and Vibration* 2 (1973) 175–183.
[2] K.M.A. Kamash, J.D. Robson, Implications of isotrophy in random surface, *Journal of Sound and Vibration* 54 (1977) 1–13.
[3] G. Rill, The influence of correlated random excitation processes on dynamics of vehicles, in: J.K. Hedrick (Ed.), *Proceedings of the Eighth IAVSD Symposium on the Dynamics of Vehicles on Roads and on Railway Tracks*, 1983, pp. 449–459.
[4] E.K. Bender, Optimization of the Random Vibration Characteristics of Vehicle Suspensions Using Random Process Theory, ScD Thesis, MIT, Cambridge, MA, 1967.
[5] A.G. Thompson, An active suspension with optimal linear state feedback, *Vehicle System Dynamics* 5 (1976) 187–192.
[6] D. Hrovat, Application of optimal control to advanced automative suspension design, *Journal of Dynamical Systems, Measurement and Control* 115 (1993) 328–342.
[7] R.M. Chalasani, Ride performance potential of active suspension systems—part I: simplified analysis based on a quarter-car model, *ASME-AMD* 80 (1986) 187–204.
[8] D. Karnopp, Theoretical limitations in active suspensions, *Vehicle System Dynamics* 15 (1986) 41–54.
[9] M.C. Smith, Achievable dynamic response for automotive active suspensions, *Vehicle System Dynamics* 24 (1995) 1–34.
[10] A. Hać, Adaptive control of vehicle suspension, *Vehicle System Dynamics* 16 (1987) 57–74.
[11] I. Fialho, G.J. Balas, Road adaptive suspension design using linear parameter-varying gain scheduling, *IEEE Transactions on Control Systems Technology* 10 (2002) 43–54.
[12] H. Akçay, S. Türkay, Frequency domain subspace-based identification of discrete-time power spectra from nonuniformly spaced measurements, *Automatica* 40 (2004) 1333–1347.
[13] K. Sobczyk, D.B. Macvean, J.D. Robson, Response to profile imposed excitation with randomly varying traversal velocity, *Journal of Sound and Vibration* 52 (1977) 37–49.
[14] J.A. Tamboli, S.G. Joshi, Optimum design of a passive suspension system of a vehicle subjected to actual random road excitations, *Journal of Sound and Vibration* 219 (1999) 193–205.
[15] D. Karnopp, M.J. Crodby, R.A. Harwood, Vibration control using semi-active force generators, *Journal of Engineering for Industry* 96 (1974) 619–626.
[16] D. Hrovat, D.L. Margolis, M. Hubbard, An approach toward the optimal semi-active suspension, *Journal of Dynamic Systems, Measurement and Control* 110 (1988) 288–296.

[17] D. Karnopp, Active and semi-active vibration isolation, *ASME Transactions* 117 (1995) 177–185 (special 50th anniversary, design issue).
[18] D. Hrovat, Survey of advanced suspension developments and related optimal control applications, *Automatica* 33 (1997) 1781–1817.